This article has been accepted for inclusion in a future issue of this journal. Content is final as presented, with the exception of pagination.

Fine-Scaled Predictive Modeling of Road Surface Conditions and Temperature in Urban Areas

Keita Ishii, Shunsuke Ono, *Senior Member, IEEE*, Takeshi Masago, Masamu Ishizuki, Teppei Mori, and Yasushi Hanatsuka

***Abstract*— Road administrators require fine-scaled information regarding road surface conditions to ensure efficient operation during winter periods. However, conventional models offer low-resolution information at a scale comparable to meteorological meshes or the spatial configuration of road weather information systems. Additionally, few methods have been proposed for predicting road surface conditions specifically in urban areas, where roads frequently experience shading from surrounding buildings. This study proposes a statistical approach for predicting road surface temperature and conditions in urban road networks. The complicated accumulated distribution of solar radiation along each road is calculated and used as an effective explanatory variable that considers the complex shading effects of nearby structures. The proposed model adopts a Bayesian spatiotemporal hierarchical framework for predicting road surface temperature using a solar radiation variable. Furthermore, a spatial machine learning model is implemented to estimate road surface conditions. The model classifies icy road conditions into six distinct types, achieving a sensitivity of 0.7712 and a balanced accuracy of 0.8637. Ultimately, the model provides significant information required for decision-making processes aimed at ensuring efficient winter road management. These results indicate that the applicability of the proposed approach can extend beyond the studied area, demonstrating its potential for broader implementation.**

***Index Terms*— Road surface temperature, road surface conditions, solar radiation, Bayesian hierarchical model, spatiotemporal model, machine learning, winter road operations.**

I. Introduction

ROAD surface weather conditions such as snow and ice significantly affect driving conditions, which can lead to serious accidents [1]. Therefore, providing and maintaining safe driving conditions on roads in urban areas is a formidable challenge for road administrators; these challenges are often characterized by complicated road networks and rapidly varying weather conditions [2], [3]. To mitigate these risks, road administrators often rely on precise and timely forecasts of road weather for optimizing snow-plowing routes, fleet sizes, and courses of sprinkling de-icing agents. Several maintenance decision support systems (MDSSs) have been developed for winter roads, particularly in cold regions [4], [5], [6]. An MDSS uses a combination of several data sources, such as weather stations, road weather information systems (RWIS), traffic sensors, and historical records of road maintenance operations, to provide accurate predictions of road weather to road agents and to offer valuable recommendations for optimal maintenance operations. Efficient operations can help reduce the economic burden on local authorities and the environmental impact caused by de-icing chemicals.

However, existing methods cannot be fully employed in practical operations because their spatial resolutions are coarser than the actual range of winter road operations [7]. This can be attributed to the significant variations in road weather conditions within a relatively small area, compared to that with weather meshes and the arrangement of RWIS. In urban areas, accurate forecasting becomes an arduous task because of the shading effect of buildings and roadside trees [8], [9]. The spatial distribution of solar radiation on road surfaces can considerably vary road weather conditions over a short range. In addition, road weather conditions change easily because of traffic conditions and the effect of heat emitted from car tires and engines [10]. Snow often does not melt easily on local, low-traffic, and narrow roads. Therefore, a method that considers local spatial variations in road weather and other significant factors is required to ensure urban road maintenance.

Thus far, we propose a framework to provide accurate road surface condition (RSC) predictions with a high spatial resolution for urban areas. This study makes three main contributions. First, the proposed model incorporates the solar radiation characteristics of each road link by considering the accumulated spatial distribution of solar radiation. Second, the spatiotemporal structure of the road surface temperature (RST) is considered for enhancing the prediction performance of the RST model. A fine-scale prediction of the RST was obtained. Third, the proposed method offers an accurate prediction of RSCs with a high resolution by using the predicted RST results.

The remainder of this paper is organized as follows. Section II presents a review of the relevant literature. Section III details the proposed model. Section IV presents the

Manuscript received 26 September 2023; revised 6 March 2024 and 7 May 2024; accepted 11 July 2024. The Associate Editor for this article was Z. Cao. *(Corresponding author: Keita Ishii.)*

Keita Ishii is with the Department of Computer Science, School of Computing, Tokyo Institute of Technology Yokohama, Kanagawa 226-8503, Japan, and also with the Digital AI/IoT Planning and Development Division, Bridgestone Corporation, Tokyo 104-8340, Japan (e-mail: ishii.k.at@m.titech.ac.jp).

Shunsuke Ono is with the Department of Computer Science, School of Computing, Tokyo Institute of Technology, Yokohama, Kanagawa 226-8503, Japan.

Takeshi Masago, Masamu Ishizuki, Teppei Mori, and Yasushi Hanatsuka are with the Digital AI/IoT Planning and Development Division, Bridgestone Corporation, Tokyo 104-8340, Japan.

Digital Object Identifier 10.1109/TITS.2024.3433004

© 2024 The Authors. This work is licensed under a Creative Commons Attribution 4.0 License.
For more information, see https://creativecommons.org/licenses/by/4.0/

This article has been accepted for inclusion in a future issue of this journal. Content is final as presented, with the exception of pagination.

validation of this model using actual measured data. Section V discusses the obtained results in detail. Finally, Section VI concludes the paper and discusses future research directions.

II. Related Works

The RST is the most important explanatory variable for accurately predicting the RSC required to achieve efficient winter road maintenance.

A. Previous Models for RST

Thus far, several RST models have been proposed because RST prediction is an important step in civil engineering, and it is imperative for winter road maintenance. Further, these models can characterize the properties of asphalt; therefore, they are used for pavement design and analysis. The predictive models of the RST can be classified into analytical and empirical models. The former is based on physical laws and explicitly represents the mechanisms that affect the RST [11], [12], [13], [14], [15]. The analytical model considers a one-dimensional (1-D) heat balance on the road surface. Weather and human activity, including the effects of traffic, induce a heat flux on the road surfaces; then, the surface emits heat into the air. In addition, it transfers heat in the depth direction because of thermal diffusion. A 1-D heat conduction differential equation was solved in the depth direction with appropriate boundary conditions to estimate the RST. The boundary condition is typically a heat-balance equation. An analytical model is complex and requires many parameters that cannot be obtained from meteorological data [16]. Therefore, the most crucial issue of the urban road weather model is fine-scale parameterization because it may be difficult to obtain detailed parameters that vary over a short range.

Several empirical models have been proposed to circumvent this difficulty. Many researchers have adopted multiple linear or nonlinear regression models for RST prediction [17], [18], [19]. For example, Chapman et al. [20] evaluated the importance of five explanatory variables (altitude, sky-view factor, road type, land use, and cold-air advection) using a multiple regression analysis. These five variables explain approximately 75% of the variation. Sreedhar and Biligiri [21] used a linear regression model to consider physical phenomena and included not only weather variables but also physical constants such as the heat capacity and thermal conductivity of the road as explanatory variables.

Statistical methods besides multiple regression analyses have been widely researched; for example, the statistical ensemble approach [22], least absolute shrinkage and selection operator [23], random forest (RF) [23], and gradient boosting regression tree [23]. Neural network models are frequently used for time-series regression tasks [24]. Shao [25] used unique explanatory variables such as variations in atmospheric temperature, differences in atmospheric temperature from one time point before, and RSC. Liu et al. [26] adopted a learning machine, which is a type of neural network, and reported that it appropriately selected activation functions. ReLU and SoftPlus enhanced the performance of the model. However, using statistical methods such as machine learning and neural networks, which are black-box approaches, can reduce the explanatory power of the models.

Few models incorporate temporal or spatial structures. Conventional models focus on the prediction of RST at a single location (in many cases, at the RWIS location). Feng and Fu [27] forecasted the RST using an autoregressive moving average with an exogenous input model and derived models incorporating various explanatory variables such as weather, traffic, and maintenance. For the spatial relationship, Berrocal et al. [28] created a Gaussian process (GP)-based model that considers the spatial dependence of the RST calculated using semi-variograms for winter mountain road maintenance. Kwon and Gu [29] obtained road weather data from a measurement vehicle and proposed an interpolation method for the RST using spatial kriging. The GIS technique is useful for spatially mapping the RST [30].

As indicated by the existing literature cited above, only some empirical models consider both the spatial and temporal structures of the RST for enhancing performance, although several models have been proposed in other fields of traffic engineering [31]. Further, only a few prediction methods can be applied in urban areas, where the spatial distribution of solar radiation is complicated because of the shading of buildings.

B. Conventional RSC Models

Conventional methods that discriminate RSC as a classification task are presented. Some models can estimate the RSC on a rule basis by predicting the RST and considering the presence of moisture on the road surface. For example, Saegusa and Fujiwara [32] created a method that predicted the RST beforehand and then determined the RSC using a rule-based approach. The authors predicted the conditions using sky conditions, ambient temperature, and RST. Recently, machine learning approaches have been widely used to solve such tasks. Many studies feed weather and traffic data into machine learning models to enhance classification accuracy. An ensemble tree-based approach was adopted to identify six different RSCs using data measured by sensors attached to vehicle tires [33]. Takasaki et al. [34] proposed an RF model to classify RSCs using RWIS data. Ishizuki et al. [35] proposed a multimodal classification model that combines a convolutional neural network with tire sensing.

However, the conventional methods can only provide information with coarse spatial resolution, which is insufficient for practical operations. This coarser prediction resolution can be attributed to the resolution depending on data characteristics, such as the mesh sizes of the weather data and the spatial arrangement of the RWIS. Further, few models consider spatial information regarding solar radiation to implement a fine prediction for RSC. An appropriate method is required to provide fine-scale information for actual operations.

III. Proposed Model

The predictive method for RSCs includes three steps:

Step 1: The spatial distributions of the solar radiation incident on the road surfaces are calculated using GIS software.

This article has been accepted for inclusion in a future issue of this journal. Content is final as presented, with the exception of pagination.

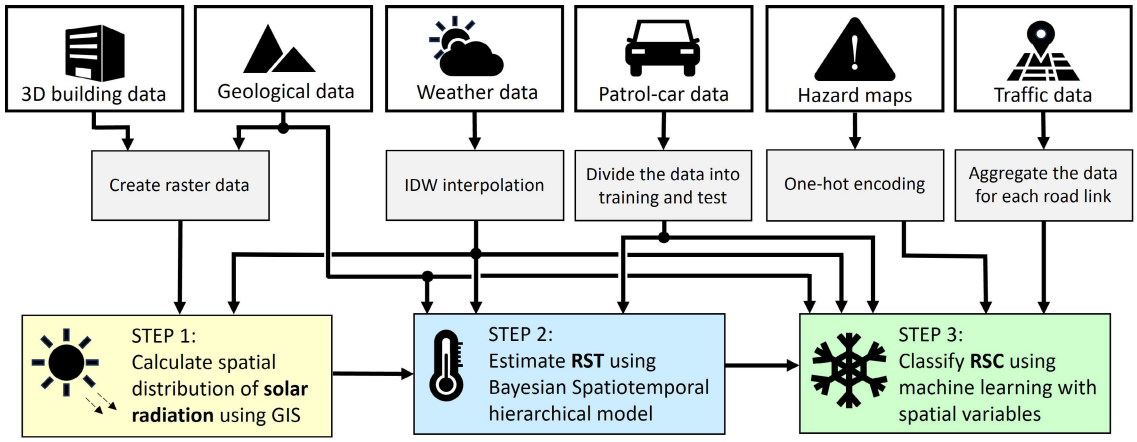

Fig. 1. Flow of the prediction system for RSCs.

Fig. 2. Example of the 3-D view of building data.

This calculation considers the shading effect of urban buildings and the azimuth of the sun.

Step 2: Bayesian spatiotemporal hierarchical models are used to predict the RST for each road link using the calculated solar radiation variable.

Step 3: The RSC is classified using spatial machine learning models with both solar radiation and RST.

The various types of data fed into the prediction model included 3-D building data for calculating the spatial distribution of solar radiation. Geographic, meteorological, and traffic data, which affect the road weather, were input into the model. Further, hazard maps (inland water and flood risk) published by the local government were used as explanatory variables to identify areas on the road that were prone to water accumulation and freezing. The flow of the proposed method is illustrated in Fig. 1.

A. Calculation of Solar Radiation Variables

GIS was used to compute the complicated spatial distribution of solar radiation on roads in urban areas. First, 3-D building data, which were polygon data, as shown in Fig. 2, were converted to raster data, including height information. Digital elevation model (DEM) data were then transformed into raster data using the inverse distance weighting (IDW) interpolation. Subsequently, the raster data were merged. Using the raster data, the spatial distribution of solar radiation on each road link was calculated using the ArcGIS solar radiation toolset of ArcGIS [36]. Furthermore, solar radiation was calculated by measuring the position of the sun every 3 h from 0:00 to 24:00 on January 1, 2022, and the total amount of solar radiation was plotted on a map. Because this calculation is costly, the plot was based only on data collected on a specific day. The diffusion proportion was set to 0.2, assuming clear skies. Details of the data we used are described in Section IV-B.

The calculation results for the solar radiation distribution poking through the buildings were converted as the explanatory variables for each road link. The distributions were overlaid on a road map to create raster data, and they were clipped to each road link based on road geometry. Histograms of the accumulated solar radiation for the roads were plotted from the raster data. The median, variance, skewness, and kurtosis of the distributions were used as the potential explanatory variables selected in a stepwise manner.

The calculations of the spatial distribution of solar radiation provides information on a road link-by-link basis, which can be used for forecasts with a sufficiently high resolution for snow removal operations. This is because many of the conventional prediction models discussed in Section II use solar radiation data from the few meteorological observation facilities located in the target area or the solar radiation data provided by a meteorological mesh. Consequently, predicting RST and RSC at the road link level becomes challenging.

However, this method has some limitations in that calculating solar radiation over a wide area is extremely time-consuming. Therefore, the calculations are repeated for small rectangular areas, which leads to discontinuous solar radiation values at the boundaries between the rectangles. In addition, the buildings are assumed to be rectangular in shape, which can cause errors in the solar radiation computation.

B. Bayesian Spatiotemporal Hierarchical Models for RST

To enhance the accuracy of RST predictions, Bayesian spatiotemporal hierarchical models were adopted. We assumed that RST adheres to the first law of geography, which posits that proximity in both time and location correlates with greater similarity in RST values. Consequently, roads situated closely to one another, even if not directly connected, should exhibit

This article has been accepted for inclusion in a future issue of this journal. Content is final as presented, with the exception of pagination.

TABLE I
BRIEF SUMMARY OF RST PREDICTION MODELS

Model	Equation	Description	Reference
Linear regression	$Y = \sum_j^p x_j\beta_j + \varepsilon$	This model is considered as the control model.	
Separable model	$Cov(e(s_i,t_k),e(s_j,t_l))$ $= \sigma^2\rho_s(\lvert s_i - s_j\rvert;v_s)\rho_t(\lvert t_k - t_l\rvert;v_t)$	This covariance model can be expressed as a product of purely spatial and temporal covariances. $\rho_s(\cdot)$ and $\rho_t(\cdot)$ are isotropic correlation functions in space and time, respectively, where vs and vt are the parameters. $\lvert s_i - s_j\rvert$ denotes the distance between sites s_i and s_j. Similarly, $\lvert t_k - t_l\rvert$ denotes the time lag between t_k and t_l. σ^2 is a constant.	[38]
Marginal model	$Y_t \sim N(\mu_t, \sigma_\epsilon^2 I + \sigma_w^2 S_w)$	This spatiotemporal hierarchical model is written as $Y_t \lvert w_t \sim N(\mu_t + w_t, \sigma_\epsilon^2 I)$, $w_t \sim N(0, \sigma_w^2 S_w)$. The random effects w_t can be marginalized out to reduce the number of sampling parameters. $\sigma_\epsilon^2 I + \sigma_w^2 S_w$ refers to the covariance matrix of the marginal distribution of Y_t.	[37]
Hierarchical centering	$Y(s_i,t) = O(s_i,t) + \epsilon(s_i,t)$, $O(s_i,t) = x^T(s_i,t)\beta + w(s_i,t)$	Used to improve the efficiency of the MCMC calculation. $O(s_i,t)$ represents the mean and random effects to which hierarchical centering is applied.	[39]
Autoregressive (AR) model	$O(s_i,t)$ $= \rho O(s_i,t-1) + x^T(s_i,t)\beta + w(s_i,t)$	In addition to the hierarchical centering, first-order temporal dependence was introduced. ρ is a constant, $0 \leq \rho \leq 1$, and if $\rho = 0$, this equation is equivalent to the hierarchical centering model.	[40]
Gaussian predictive process (GPP) model	$Y(s_i,t) = x^T(s_i,t)\beta + AO(s_i,t) + \epsilon(s_i,t)$, $O(s_i,t) = \rho O(s_i,t-1) + w(s_i,t)$ $w(s_i,t) \sim N(0, \sigma_w^2 S_{w^*})$	To reduce the calculation cost, this model considers a smaller number of sites called knots than data sites. S_{w^*} is the $m \times m$ matrix. $A = CS_{w^*}^{-1}$ and C is the cross-correlation matrix of $n \times m$. The number of knots, m, is less than the actual number of sites observed in the data, n, i.e., $m \ll n$.	[41]
Spatially dynamic model	$\beta_j(s_i,t) = \beta_{j0} + \beta_j(s_i)$	A spatially dynamic regression coefficient is adopted in this model. β_{j0} refers to the intercept and $\beta_j(s_i)$ is only dependent on the sites.	[42]
Temporally dynamic model	$\beta_j(s_i,t) = \rho\beta_j(t-1) + \delta_j(t)$	This model considers the temporally dynamic regression coefficient and has the first-order temporal dependence. $\delta_j(t)$ is the residual.	[42]

similar RST values. The parameters of these models are estimated using the Markov chain Monte Carlo (MCMC) method. In this section, we provide a concise overview and an explanation of the fundamental structures of the eight models listed in Table I, which include one linear regression, one separable, and six spatiotemporal hierarchical models.

The first level of the spatiotemporal hierarchical model is expressed as [37]

$$Y(s_i,t) = \boldsymbol{\mu}(s_i,t) + e(s_i,t), \tag{1}$$

$$\boldsymbol{\mu}(s_i,t) = \boldsymbol{x}^T(s_i,t)\boldsymbol{\beta}(s_i,t) = \sum_j^p x_j(s_i,t)\beta_j(s_i,t), \tag{2}$$

where $Y(s_i,t)$ represents the RST at the i-th site s_i and time t; $i = 1,\cdots,n$ and $t = 1,\cdots,T$. The site is expressed as the latitude and longitude of the mid-point of the road link. Further, $\mu(s_i,t)$, $e(s_i,t)$, $x(s_i,t)$, $x_j(s_i,t)$, $\beta_j(s_i,t)$, and p represent the spatiotemporal process that represents the average structure of the data, an error term, a vector of the explanatory variables, the j-th explanatory variable, the j-th regression coefficient, and the number of explanatory variables, respectively.

$e(s_i,t)$ can be interpreted to model spatiotemporal processes, and it is assumed as a spatiotemporal GP, with a mean of zero; it is flexible for modeling a spatiotemporal structure.

To model more complex spatiotemporal structures, a spatiotemporal random effect was adopted. The error term $e(s_i,t)$ can be expressed as two separate terms.

$$e(s_i,t) = w(s_i,t) + \epsilon(s_i,t), \tag{3}$$

where $w(s_i,t)$ and $\epsilon(s_i,t)$ represent the measurement errors, both of which have mean values of zero. A random effects model was used to model the spatiotemporal dependence of the data. The measurement error that follows $\epsilon(s_i,t) \sim N(0,\sigma_\epsilon^2(t))$ is assumed to be independent of the site, time, and random effect. Furthermore, there is a difference in the variance at each time point. The variance is expressed as $\sigma_\epsilon^2(t)$.

The third level of the spatiotemporal model indicates prior distributions of the parameters and hyper-parameters. Here, we used noninformative distributions as prior distributions.

To fit the RST data, several R packages, including bmstdr [37], spTimer [41], spTDyn [42], rstan [43], and spBayes [44], were used to estimate the parameters using the MCMC method. The bmstdr package is a wrapper class for other packages and is used as the main package, whereas the

This article has been accepted for inclusion in a future issue of this journal. Content is final as presented, with the exception of pagination.

TABLE II
EXPLANATORY VARIABLES INCORPORATED INTO RST AND RSC PREDICTION MODELS

Variable	Description	RST	RSC
Air temperature	Hourly data	✓	✓
Relative humidity	↑	✓	✓
Wind speed	↑	✓	✓
Sunshine duration	↑	✓	✓
Precipitation	↑		✓
Snowfall	↑		✓
Snow coverage	↑		✓
Dew point temperature	↑		✓
Air pressure	↑		✓
Visibility	↑		✓
Traffic volume	Vehicle counts for 6 hours		✓
Speed	Average speed for 6 hours		✓
Travel time	Average travel time for 6 hours		✓
Elevation (DEM)	Height above sea level	✓	✓
Road Network	Adjacent matrix		✓
Inland water map	Raise a flag at road links with this hazard		✓
Flood risk map	↑		✓
Solar radiation	Moments calculated from the distribution of solar radiation	✓	✓
Solar radiation : sunshine duration	the interaction between median of the solar radiation and sunshine duration	✓	✓
RST	Predicted RST		✓

other packages are used individually when detailed settings are required.

The use of a spatio-temporal model to predict RST facilitates the integration of temporal relationships with historical RST values and spatial structure that are neglected in the heat balance models, thereby enhancing the estimation accuracy. The road surface temperature on a particular road is assumed to be similar to the value at a nearby point in time. Moreover, even if the road is not directly connected to that road, RST is considered to be similar to the value in case the road is nearby. Consequently, the spatio-temporal model can explicitly incorporate these relationships into the model.

C. Classification Models for RSC

Six road weather conditions that are significant for winter road maintenance were classified using machine learning models based on weather variables, traffic conditions, and geographic information. Explanatory variables incorporated into this model are presented in Table II. Further, the road network of the course was incorporated into the model because the RSC can vary significantly depending on the traffic volume, even on adjacent roads. We assumed that the spatial structure of the RSC data was based on the road network, instead of the distance-based relationships assumed in the RST model. Spatial machine learning models were adopted to consider the spatial structure. These models are divided into two types [45]: The first type uses explanatory variables with spatial structures, and the other model is trained on the spatial structure. This study employed the former approach.

The road network is transformed into an adjacent matrix and used as the explanatory variable. The calculated distributions of the accumulated solar radiation are also used because snow can melt to some extent and change to slush in places where the sun shines even though the RST does not change significantly.

This study adopted six spatial machine learning models to solve the RSC classification task and compared the performance of these models. The models included support vector machines (SVMs) with radial basis function kernels [46], RFs [47], feed-forward neural networks with a single hidden layer (nnet) [48], eXtreme Gradient Boosting (XGBoost) [49], scalable weighted subspace RFs [50], and logistic model trees (LMTs) [51]. These six machine learning models were selected due to their proven efficacy in other classification tasks and their ability to capture the nonlinear structure of data. The computations were executed using the caret package in R [52], with the explanatory variables being fed in a consistent manner.

Spatial machine learning models facilitates the flexible input of spatial variables such as road network and traffic volume. Road surface conditions are not necessarily similar on roads that are close to each other; however, they are expected to be similar when roads are connected with traffic flowing through them.

IV. EXPERIMENT

A. Problem Setting

Let us assume that a patrol car regularly patrols the area to maintain winter road surfaces; however, this patrol car cannot monitor all roads because of cost and time constraints. Therefore, in addition to the data acquired by the patrol car, the RST and RSC must be spatially interpolated on roads that are not patrolled.

B. Data

A patrol car was driven around the course to measure the RST and RSC. The vehicle was equipped with various measurement instruments. For example, a radiation thermometer (Snowtech Niigata, RTM-002) was mounted on the bumper in front of the vehicle to measure the RST, and a GPS sensor (Pioneer, GPS-M1ZZ) was used to record the driving position. The vehicle was occupied by two people, a driver and measurer, who visually determined the six types of RSCs and input the data into a PC mounted in the vehicle. The data were recorded approximately every 2 m. To ensure consistent visual assessments of the RSCs, we provided thorough training to our measurers and shared our criteria for determining the RSC.

The measurements were conducted in both urban and mountainous areas in Aizuwakamatsu, Japan. Aizuwakamatsu is one of the major cities in the Tohoku region with heavy snowfall. The course is managed by a local road administrator for actual winter road operations. Fig. 3 shows the course, which is approximately 50 km long, and the number of road links.

This article has been accepted for inclusion in a future issue of this journal. Content is final as presented, with the exception of pagination.

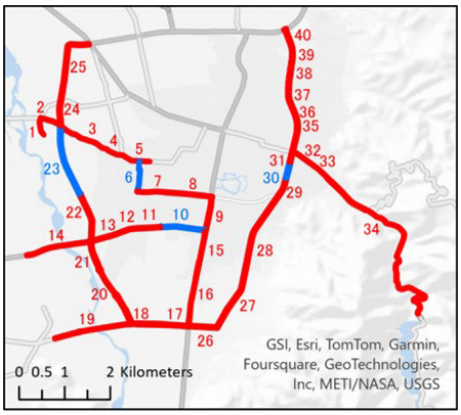

Fig. 3. Measurement course and road link numbers in Aizuwakamatsu city. A number indicates the road link number. The four roads in blue will be discussed as examples of the analytical method.

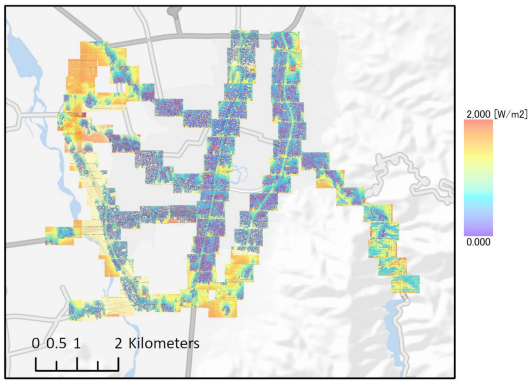

Fig. 4. Calculation results of accumulated solar radiation in Aizuwakamatsu.

A road link is a road between two nodes, i.e., an intersection, with main and arterial roads; each road link is numbered 1–40. The test was conducted for approximately four months, from December 13, 2021 to March 31, 2022. Measurements were performed three times, once every Monday and on weekends, at approximately 10:00 am, 6:00 pm, and 00:00. The size of measured RST and RSC data was 334,928.

The measured RST and RSC data were aggregated based on the number of roads in each road link to use the positioning accuracy problem of the GPS, which caused a deviation of several hundred meters from the actual results. The deviations were corrected by simple map matching because the measurement vehicle traveled on the nearest road link. The RST is the average value within a road link, RSC is defined as a mode condition, and the location of the road link is defined as its mid-point. Ultimately, the data size was changed into 2,048.

There are missing values in the data because of cancellations caused by the unusually heavy snowfall and other safety issues that arose during the test period or because the course was shortened. Further, some data storage failed because of an Internet glitch. The missing data were input using the average of the measured values for the same travel.

Meteorological data were extracted from hourly data obtained from three observatories (Wakamatsu, Inawashiro, and Kanayama) near the course; these data are publicly available from the Japan Meteorological Agency. The IDW interpolation method was used to calculate the weather conditions at the mid-point of each road link. The detailed weather variables are presented in Table II.

Several maps of the Aizuwakamatsu area were incorporated in addition to weather data. The maps were drawn using ArcGIS. The data for the 3-D buildings in Fig. 2 and road maps in Fig. 3 were obtained from the ArcGIS Stat Suite. The Geospatial Information Authority of Japan provided the 5-meter-mesh DEM. The road traffic statistics computed by ArcGIS were used for obtaining the traffic volume, travel time, and vehicle speed data every 6 h for each road. Hazard maps for inland water and flood risks published by the Aizuwakamatsu city government were used to highlight the locations on each road link where water accumulated. These variables were incorporated into the model as binary explanatory variables for each road link. A summary of the explanatory variables input into our model is presented in Table II.

C. Model Validation

Of the RST and RSC data obtained from the patrol car, 87.5% was used as training data and the remaining 12.5% as test data. Our model was trained using the training data and evaluated based on its predictive performance on the test data. The predictions were computed at a road-link scale, which is particularly relevant for winter road operations. To assess the performance of the RST models, several metrics were employed, namely the goodness of fit (GOF), predictive model choice criteria (PMCC) [53], root mean square error (RMSE), and mean absolute error (MAE). Similarly, four metrics were used to evaluate the RSC models with respect to the ice condition: accuracy, sensitivity, precision, and balanced accuracy. In this experiment, the occurrence of ice conditions was associated with relatively rare but harmful events. Balanced accuracy, which can be expressed as $Balanced\ accuracy = \frac{1}{2} \cdot (Sensitivity + Precision)$, is a particularly useful metric for tasks involving imbalanced data; hence, it was deemed essential for evaluating the ice condition predictive performance in this study.

D. Accumulated Spatial Distributions of Solar Radiation

The amount of solar radiation incident on the course was computed by considering the shading effect of the surrounding buildings, as shown in Fig. 4. Fig. 4 presents the results for Aizuwakamatsu. The maps on the left-hand side of Fig. 5 illustrate four specific locations: Road links 6, 10, 23, and 30. In these maps, areas exposed to stronger solar radiation are indicated in yellow and red, whereas the weaker areas are indicated in blue and purple. The color bar of these maps is shown in Fig. 5 (a1).

Histograms of the accumulated solar radiation of the four road links are also illustrated in Fig. 5 from (a2) to (d2), which were calculated from the clipped maps shown on the left-hand side of Fig. 5 according to the shape of the road links. Road links 6 and 10 had lower solar radiation because the roads were narrow and passed through residential areas. In contrast, road links 23 and 30 received more solar radiation; there were few

This article has been accepted for inclusion in a future issue of this journal. Content is final as presented, with the exception of pagination.

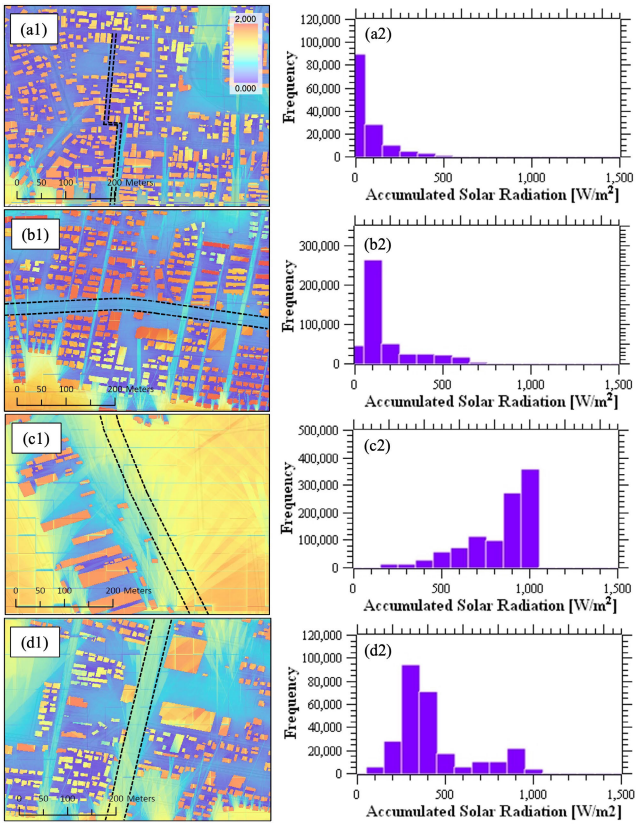

Fig. 5. Maps of accumulated solar radiation around (a1) road links 6, (b1) 10, (c1) 23, and (d1) 30. The dashed line represents a road link in each map. The color bar in (a1) is common to the other three maps. The four histograms from (a2) to (d2) show distributions of accumulated solar radiation for the same roads as the maps shown to the left of them.

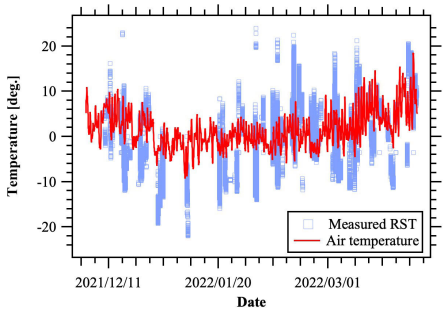

Fig. 6. Measured RST (raw data) in Aizuwakamatsu city course and air temperature observed by the Wakamatsu observatory in the course.

buildings around road link 23, and road link 30 went through the city center; however, the road was relatively wide. These graphs illustrate the characteristics of each road link. With an increase in the amount of accumulated solar radiation, the RST may increase and the conditions provided by RSC may improve.

E. RST Prediction

The experimental data measured by the patrol car during the experimental period is shown in Fig. 6. This graph shows the air temperatures observed by the Wakamatsu observatory located within the patrol course. Air temperature exhibited a trend similar to that of the RST. The temperature values gradually decreased from December 2021 to January 2022. Although the air temperature was stable in January and February 2022, the RST exhibited the lowest values. However, they both exhibited increasing trends in March 2022. The RST tended to be lower in mountainous areas, i.e., the high-elevation area located in the southeastern part of Aizuwakamatsu (road link 34).

TABLE III
PERFORMANCES OF MODELS FOR PREDICTING THE RST

Model	GOF	PMCC	RMSE	MAE
Linear regression (control)	867.4	1754.5	1.90	1.47
Separable model	207.1	370.2	3.01	2.71
Marginal model	154.9	**309.0**	**0.39**	**0.31**
Hierarchical centering	196.1	847.9	0.55	0.43
AR model	194.4	833.8	0.55	0.42
GPP model	**84.6**	398.5	**0.39**	**0.32**
Spatial dynamic model	191.1	394.5	0.53	0.43
Temporal dynamic model	200.6	690.0	0.56	0.44

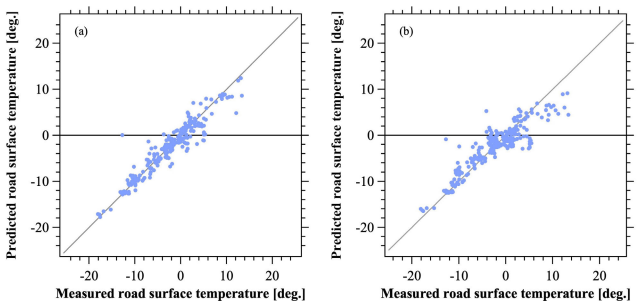

Fig. 7. Comparisons of measured RST with the one predicted using (a) the marginal model and (b) GPP model.

A performance comparison of the various spatiotemporal models is summarized in Table III. Compared to the control model, which is a linear regression, the spatiotemporal random effect models outperformed the other models. The simple separable model performed poorly considering that a complex spatiotemporal structure is effective for improving the prediction accuracy for this task. The marginal model exhibited the best performance in terms of these metrics partly because this model has fewer parameters to estimate, compared to the other models. The GPP model had the lowest GOF value and was comparable to the marginal model in terms of the RMSE and MAE. Fig. 7 shows the comparisons of the predicted RST with the measured RST of the marginal model; the GPP mode was implemented. These graphs illustrate that these two models showed good predictive performances; however, the marginal model achieved slightly better results than the GPP model.

F. Performances of RSC Models

Six conditions were classified for each road link using various explanatory variables such as the predicted RST obtained in the previous subsection; traffic, weather, and geographical data; and road networks. These explanatory variables are based on road links. We compared six different machine learning classifiers to select the best model. All input explanatory variables were the same.

This article has been accepted for inclusion in a future issue of this journal. Content is final as presented, with the exception of pagination.

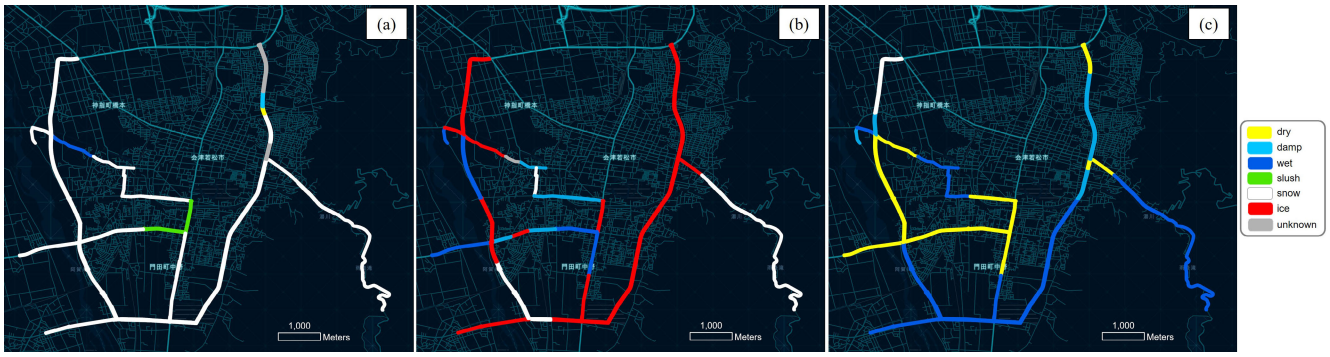

Fig. 8. Road condition maps: (a) at 00:12 (JST) on Feb. 7th, (b) at 20:53 on Feb. 7th, and (c) at 14:27 on Feb. 8th.

TABLE IV
PERFORMANCES OF MACHINE LEARNING MODELS FOR CLASSIFYING THE RSC

Model	Accuracy	Sensitivity (ice)	Precision (ice)	Balanced Accuracy (ice)
SVM	0.6458	0.5357	0.9506	0.7432
RF	**0.7897**	0.7200	0.9634	0.8417
nnet	0.5609	0.3571	0.9476	0.6524
XGBoost	0.7712	**0.7600**	**0.9675**	**0.8637**
WSRF	0.7823	0.6923	0.9633	0.8278
LMT	0.7306	0.6539	0.9592	0.8065

The comparison results in Table IV indicate that XGBoost is the best model for this task because it exhibits the highest sensitivity and balanced accuracy with respect to ice.

Next, for a more detailed analysis, we compared the prediction performances of these machine learning models using RSC data from the night of February 6, 2022 to the evening of February 8, 2022. This is because the RSC changed rapidly during this short period, and all six conditions occurred.

Fig. 8 illustrates the maps showing the transition of the RSC prediction during this period and is an example of the output of this system. At 00:12 on February 7, almost the entire course was covered with snow, as shown in Fig. 8(a). During daytime, owing to sunlight, the snow surface melted into a damp condition. Later, during the night the RSC changed into the icy condition shown in Fig. 8(b). The next day, the ice melted again under the influence of the sun, and the road surface gradually dried out (Fig. 8(c)).

Fig. 9 shows graphs comparing the top four machine learning methods with respect to accuracy: (a) SVM, (b) RF, (c) nnet, (d) XGBoost, (e) WSRF, and (f) LMT. These graphs are the results of predicting test data randomly selected from the RSC data for this period. In Fig. 9, labels are shown as gray bars, and colored plots indicate the prediction results for each model. Red plots indicate incorrect predictions. These graphs show how each model missed its predictions. All models tended to have relatively high prediction performances on snowy and icy conditions. Although it is essential to have high classification accuracy, it is undesirable to erroneously classify adverse road surface conditions as dry, from a practical point of view. In this respect, XGBoost and RF are better than other models.

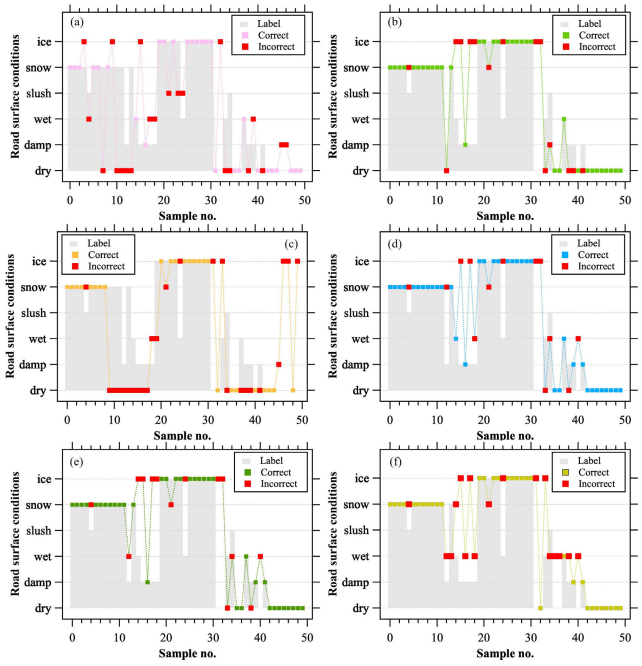

Fig. 9. Prediction results of machine learning models between the night of February, 6 and mid-night of February, 8: (a) SVM, (b) RF, (c) nnet, (d) XGBoost, (e) WSRF, and (f) LMT. Gray bars represent the labels, and colored plots refer to the predicted RSC. The red points represent incorrect predictions, whereas the others indicate correct predictions.

The bottleneck with respect to the computational efficiency in this method is the machine learning training time. The solar radiation calculation is considerably time consuming; however, it can be pre-computed. In addition, all the RST spatio-temporal models require only a few tens of seconds to train. XGBoost, the most accurate model, required 4175.51 s, or approximately 1.16 h to train. In contrast, RF was computationally lighter, requiring 684.23 s, or approximately 0.19 h. In this problem setting, the patrol car should be driven at least 1 h prior to the snow ploughing operations to obtain actual road surface condition data. This is operationally feasible.

V. DISCUSSION

This study devised a method for predicting the RST using Bayesian spatiotemporal hierarchical models considering the distributions of accumulated solar radiation and for predicting the use of machine learning models with spatial explanatory

This article has been accepted for inclusion in a future issue of this journal. Content is final as presented, with the exception of pagination.

variables. This model provides fine-scale RSC information for each road link. Although the incorporation of solar radiation into RST prediction models for urban areas is important, many existing models have used it in a limited manner. Diefenderfer et al. [54] considered the position of the sun, which affects the amount of solar radiation; however, the authors calculated the solar radiation that decreased to a certain point where they aimed to predict the RST. In addition, only some models consider the effects of buildings and trees [8] and sky-view factors [55]. Our method overcomes the shortcomings of conventional models by considering the spatial distribution of solar radiation, which is precisely calculated using GIS software. In Figs. 4 and 5, the maps clearly demonstrate changes in the shading effect of buildings according to the position of the sun. Fig. 5 (a1) and (b1) show roads that pass through residential areas, thus receiving a lower amount of sunlight, even though they may shine through the buildings to the roads when the sun is in a certain position. These are observed as streaks of light on the map. In contrast, Fig. 5 (c1) shows an open area that receives sunlight for most of the day. Fig. 5 (d1) indicates that wide roads extending to the north from the south receive a relatively larger amount of solar radiation. Fig. 5 (a2) through (d2) confirm the variation in the solar radiation for each road link.

As per the RST prediction, the marginal model performed well when estimating the RST in terms of the four metrics (Table III) because it has fewer parameters than others and because the random effects are integrated. The GPP model also exhibited a good performance. This model assumes first-order temporal dependence and considers the spatial autocorrelation of the grid of knots, rather than that of all data. This intentionally reduced the number of sites to be considered, which might have resulted in better convergence during the estimation. In other models, a separable model may indicate that RST prediction must be assumed to have a more complex spatiotemporal structure, rather than a simple covariance, which is the product of a purely spatial and purely temporal covariance. Hierarchical centering reduces the estimation time of parameters; however, its performance is poor. For the temporal and spatial dynamic models, the convergence varied significantly depending on the regression coefficients used in the dynamic form. Only the temperature was estimated assuming dynamic regression coefficients. However, both temporal and spatial dynamic models did not perform well in this task.

Even differences in the RSCs between adjacent roads within one grid mesh of weather variables must be predicted to provide useful information for winter road operations.

In the RSC prediction task, tree-based models, specifically RFs and XGBoost, outperformed other models in terms of accuracy. We posit that sensitivity to ice conditions emerges as the most critical metric, given the profound impact of adverse road surfaces on safety. Considering that a predictive model should minimize false negatives regarding ice conditions to effectively safeguard road users, XGBoost emerged as the superior model, exhibiting the highest sensitivity (0.7712) and balanced accuracy (0.8637) for icy road surfaces, as depicted in Fig. 9. However, our findings indicate a performance level lower than that reported in prior studies, including that of the RF used by Takasaki et al. [34] to predict RSC. One potential explanation for the diminished performance of our model lies in the different nature of the tasks involved. In particular, during our experiment, models were tasked with estimating RSC with a notably higher resolution, since it is deemed that predicting RSC disparities even among adjacent roads within a single grid mesh of weather variables is essential to provide pertinent information for winter road operations.

The event history data of road operations must be incorporated to enhance the performance of RSC models. The spread of de-icing agents can continue to affect the RSC until it is completely drained from the road surface, making it difficult to predict. Fujimoto et al. [13] considered salt balance on the road surface in their prediction method. However, the proposed method had several limitations:

1) We assumed that the buildings were rectangular and did not consider trees along the roads.
2) Historical road operation data were not used in this model.
3) The positioning precision of the GPS installed on the patrol car was poor, indicating that the quality of the RST and RSC data was also poor.

This model can provide near-future forecast information (e.g., 24 h ahead) required for operational planning decisions. However, this study could not verify the forecasting performance because of the intervals between measurements and the small number of measurements; therefore, it focused on achieving spatial prediction at approximately the same time as the patrol car.

The notable findings of this study are as follows:

- Utilizing the spatial distributions of solar radiation and a Bayesian spatiotemporal hierarchical model enabled us to implement the RST prediction for each road link.
- The marginal and GPP models performed better than the other spatiotemporal models for RST prediction.
- For the RSC prediction task for each road link, the recall and balanced accuracy (ice) of XGBoost outperformed the other machine learning models.

VI. Conclusion

This study developed a framework that provides accurate RST and RSC predictions in urban areas with high spatial resolutions to improve winter road operations and traffic safety. Complex solar radiation distributions were incorporated in a city area to consider the shading effect of buildings into the prediction model for the RST using GIS. The RST was predicted using a Bayesian spatiotemporal hierarchical model with various explanatory variables such as weather. The model assumed a spatiotemporal autocorrelation in the RST. Thus, the RSC was predicted using machine learning models considering the spatial structure of the road network. Weather variables, an adjacent matrix of the road network, and traffic conditions were incorporated into the machine learning models.

The proposed method was applied to a real scenario in which a patrol car occasionally collected information; the mechanism used by the proposed model to spatially interpolate

This article has been accepted for inclusion in a future issue of this journal. Content is final as presented, with the exception of pagination.

the observation gaps was investigated. The marginal and GPP models achieved better performances for RST prediction. For predicting RSCs in dirty conditions, tree-based models such as XGBoost, delivered a high performance (sensitivity: 0.7712 and balanced accuracy: 0.8637). However, this study had some limitations. Limited data on the 3-D shapes of buildings, positions of patrol cars, and road operation history can deteriorate prediction performance.

By resolving some of the data limitations, the model becomes more useful for real-world operations. High frequency data acquisition will enable this model to predict road surface conditions with high accuracy in the near future. The use of 3D data with precise building geometry and digital surface model (DSM) data that includes 3D shapes such as street trees will improve the accuracy of solar radiation calculations [56]. The accuracy can be improved by installing a weather data observation system on patrol cars to capture local weather changes. Incorporating the operational history of snow plowing and sprinkling de-icing agents and the concentration of salinity on the road surface is important for attaining a better performance of the model. The performance of this framework will be verified in other areas, and potential applications will be studied.

REFERENCES

[1] B. Hallmark and J. Dong, "Examining the effects of winter road maintenance operations on traffic safety through visual analytics," in *Proc. IEEE 23rd Int. Conf. Intell. Transp. Syst. (ITSC)*, Sep. 2020, pp. 1–6. [Online]. Available: https://ieeexplore.ieee.org/document/9294266/

[2] K. C. Dey, A. Mishra, and M. Chowdhury, "Potential of intelligent transportation systems in mitigating adverse weather impacts on road mobility: A review," *IEEE Trans. Intell. Transp.*, vol. 16, no. 3, pp. 1107–1119, Jun. 2015.

[3] V. R. Tomás, M. Pla-Castells, J. J. Martínez, and J. Martínez, "Forecasting adverse weather situations in the road network," *IEEE Trans. Intell. Transp. Syst.*, vol. 17, no. 8, pp. 2334–2343, Aug. 2016.

[4] W. P. Mahoney and W. L. Myers, "Predicting weather and road conditions: Integrated decision-support tool for winter road-maintenance operations," *Transp. Res. Rec., J. Transp. Res. Board*, vol. 1824, no. 1, pp. 98–105, Jan. 2003. [Online]. Available: http://journals.sagepub.com/doi/10.3141/1824-11

[5] M. Nefzi, A. Marzouki, A. Hajji, S. Mellouli, and M. Rekik, "Performance-based maintenance decision support system (MDSS) in snow disposal context," in *Proc. 11th Int. Conf. Modeling, Optim. Simulation (MOSIM)*, Montreal, QC, Canada, Aug. 2016. [Online]. Available: https://www.researchgate.net/publication/305221281

[6] A. Kociánová, "The intelligent winter road maintenance management in Slovak conditions," *Proc. Eng.*, vol. 111, pp. 410–419, Jan. 2015.

[7] Transportation Research Board and National Research Council, *Where the Weather Meets the Road*. Washington, DC, USA: National Academies Press, Mar. 2004.

[8] Y. Hu, E. Almkvist, F. Lindberg, J. Bogren, and T. Gustavsson, "The use of screening effects in modelling route-based daytime road surface temperature," *Theor. Appl. Climatol.*, vol. 125, nos. 1–2, pp. 303–319, Jul. 2016. [Online]. Available: https://link.springer.com/article/10.1007/s00704-015-1508-9

[9] Y. Zhang, S. Jha, D. M. Bullock, and J. V. Krogmeier, "Generating dynamic prescription maps for winter road treatment via sun-shadow simulation," in *Proc. IEEE Int. Intell. Transp. Syst. Conf. (ITSC)*, Sep. 2021, pp. 3387–3392.

[10] A. H. Perry and L. J. Symons, *Highway Meteorology*, A. Perry and L. Symons, Eds., Boca Raton, FL, USA: CRC Press, Aug. 1991.

[11] B. H. Sass, "A numerical model for prediction of road temperature and ice," *J. Appl. Meteorol.*, vol. 31, no. 12, pp. 1499–1506, Dec. 1992. [Online]. Available: http://journals.ametsoc.org/doi/10.1175/1520-0450(1992)031<1499:ANMFPO>2.0.CO;2

[12] L.-P. Crevier and Y. Delage, "METRo: A new model for road-condition forecasting in Canada," *J. Appl. Meteorol.*, vol. 40, no. 11, pp. 2026–2037, Nov. 2001. [Online]. Available: http://journals.ametsoc.org/doi/10.1175/1520-0450(2001)040<2026:MANMFR>2.0.CO;2

[13] A. Fujimoto et al., "A road surface freezing model using heat, water and salt balance and its validation by field experiments," *Cold Regions Sci. Technol.*, vols. 106–107, pp. 1–10, Oct. 2014. [Online]. Available: https://linkinghub.elsevier.com/retrieve/pii/S0165232X14001013

[14] M. Kangas, M. Heikinheimo, and M. Hippi, "RoadSurf: A modelling system for predicting road weather and road surface conditions," *Meteorol. Appl.*, vol. 22, no. 3, pp. 544–553, Jul. 2015. [Online]. Available: https://onlinelibrary.wiley.com/doi/10.1002/met.1486

[15] C. Meng, "A numerical forecast model for road meteorology," *Meteorol. Atmos. Phys.*, vol. 130, no. 4, pp. 485–498, Aug. 2018.

[16] R. Kršmanc, A. Š. Slak, and J. Demšar, "Statistical approach for forecasting road surface temperature," *Meteorological Appl.*, vol. 20, no. 4, pp. 439–446, Dec. 2013.

[17] M. R. Islam, S. Ahsan, and R. A. Tarefder, "Modeling temperature profile of hot-mix asphalt in flexible pavement," *Int. J. Pavement Res. Technol.*, vol. 8, no. 1, pp. 47–52, 2015.

[18] A. Asefzadeh, L. Hashemian, and A. Bayat, "Development of statistical temperature prediction models for a test road in Edmonton, Alberta, Canada," *Int. J. Pavement Res. Technol.*, vol. 10, no. 5, pp. 369–382, Sep. 2017.

[19] Y. Li, L. Liu, and L. Sun, "Temperature predictions for asphalt pavement with thick asphalt layer," *Construct. Building Mater.*, vol. 160, pp. 802–809, Jan. 2018.

[20] L. Chapman, J. E. Thornes, and A. V. Bradley, "Modelling of road surface temperature from a geographical parameter database. Part 1: Statistical," *Meteorol. Appl.*, vol. 8, no. 4, pp. 409–419, Dec. 2001.

[21] S. Sreedhar and K. P. Biligiri, "Development of pavement temperature predictive models using thermophysical properties to assess urban climates in the built environment," *Sustain. Cities Soc.*, vol. 22, pp. 78–85, Apr. 2016.

[22] Z. Sokol, V. Bližňák, P. Sedlák, P. Zacharov, P. Pešice, and M. Škuthan, "Ensemble forecasts of road surface temperatures," *Atmos. Res.*, vol. 187, pp. 33–41, May 2017.

[23] B. Liu et al., "Forecasting road surface temperature in Beijing based on machine learning algorithms," in *Proc. 3rd Int. Conf. Crowd Sci. Eng.*, Jul. 2018, pp. 1–5.

[24] Z. Chen, M. Ma, T. Li, H. Wang, and C. Li, "Long sequence time-series forecasting with deep learning: A survey," *Inf. Fusion*, vol. 97, Sep. 2023, Art. no. 101819.

[25] J. Shao, "Improving nowcasts of road surface temperature by a back-propagation neural network," *Weather Forecasting*, vol. 13, no. 1, pp. 164–171, Mar. 1998. [Online]. Available: http://journals.ametsoc.org/doi/10.1175/1520-0434(1998)013<0164:INORST>2.0.CO;2

[26] B. Liu et al., "Road surface temperature prediction based on gradient extreme learning machine boosting," *Comput. Ind.*, vol. 99, pp. 294–302, Aug. 2018.

[27] F. Feng and L. Fu, "Winter road surface condition forecasting," *J. Infrastruct. Syst.*, vol. 21, no. 3, pp. 1–12, Sep. 2015. [Online]. Available: https://ascelibrary.org/doi/10.1061/%28ASCE%29IS.1943-555X.0000241

[28] V. J. Berrocal, A. E. Raftery, T. Gneiting, and R. C. Steed, "Probabilistic weather forecasting for winter road maintenance," *J. Amer. Stat. Assoc.*, vol. 105, no. 490, pp. 522–537, Jun. 2010.

[29] T. J. Kwon and L. Gu, "Modelling of winter road surface temperature (RST)—A GIS-based approach," in *Proc. 4th Int. Conf. Transp. Inf. Saf. (ICTIS)*, Aug. 2017, pp. 551–556. [Online]. Available: http://ieeexplore.ieee.org/document/8047820/

[30] L. Chapman and J. E. Thornes, "A blueprint for 21st century road ice prediction," in *Proc. 11th Standing Int. Road Weather Conf. (SIRWEC)*, 2002.

[31] D. Sun, K. Zhang, and S. Shen, "Analyzing spatiotemporal traffic line source emissions based on massive didi online car-hailing service data," *Transp. Res. D, Transp. Environ.*, vol. 62, pp. 699–714, Jul. 2018.

[32] A. Saegusa and Y. Fujiwara, "A study on forecasting road surface conditions based on weather and road surface data," *IEICE Trans. Inf. Syst.*, vol. E90-D, no. 2, pp. 509–516, Feb. 2007. [Online]. Available: http://search.ieice.org/bin/summary.php?id=e90-d_2_509&category=D&year=2007&lang=E&abst=

This article has been accepted for inclusion in a future issue of this journal. Content is final as presented, with the exception of pagination.

[33] T. Mori, T. Ohiro, Y. Hanatsuka, and T. Higuchi, "Data-driven road condition forecasting with high spatial resolution: Utilizing tire-centric road condition monitoring technology," in *Proc. IEEE 23rd Int. Conf. Intell. Transp. Syst. (ITSC)*, Sep. 2020, pp. 1–8.

[34] Y. Takasaki, M. Saldana, J. Ito, and K. Sano, "Development of a method for estimating road surface condition in winter using random forest," *Asian Transp. Stud.*, vol. 8, Jan. 2022, Art. no. 100077.

[35] M. Ishizuki et al., "Image and CAIS features-based estimation of road surface condition on winter local road," in *Proc. IEEE 11th Global Conf. Consum. Electron. (GCCE)*, Oct. 2022, pp. 79–80.

[36] P. Fu and P. M. Rich, "Design and implementation of the solar analyst: An arcview extension for modeling solar radiation at landscape scales," in *Proc. 19th Annu. ESRI User Conf.*, San Diego, CA, USA, 1999, pp. 1–31.

[37] S. K. Sahu, *Bayesian Modeling of Spatio-Temporal Data With R*. Boca Raton, FL, USA: CRC Press, 2021. [Online]. Available: https://www.taylorfrancis.com/books/9780429318443

[38] K. V. Mardia and C. R. Goodall, "Spatial–temporal analysis of multivariate environmental monitoring data," *Multivariate Environ. Statist.*, vol. 6, no. 76, pp. 347–385, 1993.

[39] A. E. Gelfand, S. K. Sahu, and B. P. Carlin, "Efficient parametrisations for normal linear mixed models," *Biometrika*, vol. 82, no. 3, p. 479, Sep. 1995. [Online]. Available: https://academic.oup.com/biomet/article/82/3/479/260514

[40] S. K. Sahu, A. E. Gelfand, and D. M. Holland, "High-resolution space–time ozone modeling for assessing trends," *J. Amer. Stat. Assoc.*, vol. 102, no. 480, pp. 1221–1234, Dec. 2007. [Online]. Available: http://www.tandfonline.com/doi/abs/10.1198/016214507000000031

[41] K. S. Bakar and S. K. Sahu, "SpTimer: Spatio-temporal Bayesian modeling using R," *J. Stat. Softw.*, vol. 63, no. 15, pp. 1–32, 2015. [Online]. Available: https://www.jstatsoft.org/index.php/jss/article/view/v063i15

[42] K. S. Bakar, P. Kokic, and H. Jin, "Hierarchical spatially varying coefficient and temporal dynamic process models using spTDyn," *J. Stat. Comput. Simul.*, vol. 86, no. 4, pp. 820–840, Mar. 2016.

[43] Stan Development Team. (2023). *RStan: The R Interface To Stan, R Package Version 2.21.8*. [Online]. Available: https://mc-stan.org/

[44] A. O. Finley, S. Banerjee, and A. E. Gelfand, "spBayes for large univariate and multivariate point-referenced spatio-temporal data models," *J. Stat. Softw.*, vol. 63, no. 13, pp. 1–24, 2015. [Online]. Available: http://www.jstatsoft.org/v63/i13/

[45] B. Nikparvar and J. C. Thill, "Machine learning of spatial data," *ISPRS Int. J. Geo-Inf.*, vol. 10, no. 9, p. 600, 2021. [Online]. Available: https://www.mdpi.com/2220-9964/10/9/600/htm

[46] B. E. Boser, I. M. Guyon, and V. N. Vapnik, "A training algorithm for optimal margin classifiers," in *Proc. 5th Annu. Workshop Comput. Learn. Theory*, Jul. 1992, pp. 144–152.

[47] L. Breiman, "Random forests," *Mach. Learn.*, vol. 45, pp. 5–32, Oct. 2001. [Online]. Available: https://link.springer.com/article/10.1023/A:1010933404324

[48] W. N. Venables and B. D. Ripley, *Modern Applied Statistics With S*, 4th ed., New York, NY, USA: Springer, 2013.

[49] T. Chen and C. Guestrin, "XGBoost: A scalable tree boosting system," in *Proc. 22nd ACM SIGKDD Int. Conf. Knowl. Discovery Data Mining*, Aug. 2016, pp. 785–794, doi: 10.1145/2939672.2939785.

[50] H. Zhao, G. J. Williams, and J. Z. Huang, "wsrf: An R package for classification with scalable weighted subspace random forests," *J. Stat. Softw.*, vol. 77, no. 3, pp. 1–30, 2017.

[51] N. Landwehr, M. Hall, and E. Frank, "Logistic model trees," *Mach. Learn.*, vol. 59, nos. 1–2, pp. 161–205, May 2005. [Online]. Available: http://link.springer.com/10.1007/s10994-005-0466-3

[52] M. Kuhn, "Building predictive models in R using the caret package," *J. Stat. Softw.*, vol. 28, no. 5, pp. 1–26, 2008. [Online]. Available: http://www.jstatsoft.org/v28/i05/

[53] A. Gelfand, "Model choice: A minimum posterior predictive loss approach," *Biometrika*, vol. 85, no. 1, pp. 1–11, Mar. 1998. [Online]. Available: https://academic.oup.com/biomet/article/85/1/1/238416

[54] B. K. Diefenderfer, I. L. Al-Qadi, and S. D. Diefenderfer, "Model to predict pavement temperature profile: Development and validation," *J. Transp. Eng.*, vol. 132, no. 2, pp. 162–167, Feb. 2006. [Online]. Available: https://ascelibrary.org/doi/10.1061/%28ASCE%290733-947X%282006%29132%3A2%28162%29

[55] L. Chapman, J. E. Thornes, and A. V. Bradley, "Modelling of road surface temperature from a geographical parameter database. Part 2: Numerical," *Meteorol. Appl.*, vol. 8, no. 4, pp. 421–436, Dec. 2001, doi: 10.1017/s1350482701004042.

[56] D. Sun and Y. Zhang, "Influence of avenue trees on traffic pollutant dispersion in asymmetric street canyons: Numerical modeling with empirical analysis," *Transp. Res. D, Transp. Environ.*, vol. 65, pp. 784–795, Dec. 2018.

Keita Ishii received the B.S. and M.S. degrees in applied physics from Keio University, Japan, in 2001 and 2003, respectively. He is currently pursuing the Ph.D. degree with Tokyo Institute of Technology, Japan. He joined Toshiba Corporation to develop a new field-emission display. In 2007, he transferred to Bridgestone Corporation, where he was involved in e-paper, rubber, and tire technology. He is conducting research on intelligent tire systems and statistical modeling as a Digital Specialist.

Shunsuke Ono (Senior Member, IEEE) received the B.E. degree in computer science and the M.E. and Ph.D. degrees in communications and computer engineering from Tokyo Institute of Technology, in 2010, 2012, and 2014, respectively.

From April 2012 to September 2014, he was a Research Fellow (DC1) of Japan Society for the Promotion of Science (JSPS). From October 2016 to March 2020, he was a Researcher of the Precursory Research for Embryonic Science and Technology (PRESTO), Japan Science and Technology Agency (JST), Tokyo, Japan, where he has been since October 2021. He is currently an Associate Professor with the Department of Computer Science, School of Computing, Tokyo Institute of Technology. His research interests include signal processing, image analysis, remote sensing, mathematical optimization, and data science.

Dr. Ono received the Young Researchers' Award and the Excellent Paper Award from IEICE in 2013 and 2014, respectively; the Outstanding Student Journal Paper Award and the Young Author Best Paper Award from the IEEE SPS Japan Chapter in 2014 and 2020, respectively; the Funai Research Award from the Funai Foundation in 2017; the Ando Incentive Prize from the Foundation of Ando Laboratory in 2021; the Young Scientists' Award from MEXT in 2022; and the Outstanding Editorial Board Member Award from IEEE SPS in 2023. He has been an Associate Editor of IEEE TRANSACTIONS ON SIGNAL AND INFORMATION PROCESSING OVER NETWORKS since 2019.

Takeshi Masago received the B.S. and M.S. degrees in mechanical engineering from Aoyama Gakuin University, Japan, in 2004 and 2006, respectively. Since 2006, he has been with Bridgestone Corporation, where he researched and developed the tire-sensing algorithm. He is currently working on the development and implementation of the tire-state monitoring systems.

This article has been accepted for inclusion in a future issue of this journal. Content is final as presented, with the exception of pagination.

Masamu Ishizuki received the bachelor's and Master of Engineering degrees from Waseda University, Tokyo, Japan, in 2010 and 2012, respectively. In 2012, he joined Bridgestone, a leading tire company, where he worked as a Production Engineer specializing in electrical systems until 2018. From 2018, he was involved in research and development focused on leveraging data science for a solutions business.

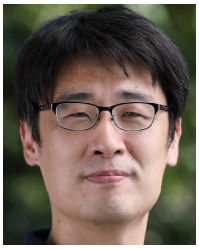

Teppei Mori received the B.S., M.S., and Ph.D. degrees in engineering from The University of Tokyo, Japan, in 2004, 2006, and 2009, respectively. In 2009, he joined Bridgestone Corporation, Japan, where he worked as an Engineer of rubber material development and rubber plantation technology development. He has been the Manager of the Digital AI/IoT Planning and Developing Division, Bridgestone Corporation, since 2020.

Yasushi Hanatsuka received the B.S. and M.S. degrees in material science from the University of Tsukuba, Japan, in 2001 and 2003, respectively, and the Ph.D. degree in statistical mathematics from the Graduate University for Advanced Studies, Japan, in 2013. He joined Bridgestone Corporation, Japan, in 2003, where he has worked as an Engineer of advanced tire development. He has been the Director of the Digital Solution AI/IoT Planning and Development Division, Bridgestone Corporation, since 2023, and a specially appointed Professor with Tohoku University, Japan, since 2021.